Trimethylsilyl-Substituted Indenyl-$TiCl_3$ Half-Sandwich Complexes: Synthesis, Solid-State Structure, and Analysis of Substituent Effects

Thomas Weiss, Uwe Böhme,*,† Bernhard Walfort, Gerd Rheinwald, and Heinrich Lang*

Technische Universität Chemnitz, Fakultät für Naturwissenschaften, Institut für Chemie, Lehrstuhl Anorganische Chemie, Strasse der Nationen 62, D-09111 Chemnitz, Germany

Received June 16, 2004

The regioselective synthesis of (η^5:2-$Me_3SiC_9H_6$)$TiCl_3$ (**4**) was effected by the reaction of $TiCl_4$ with 1,2-$(Me_3Si)_2C_9H_6$ (**3**). The solid-state structure of **4** is reported and compared with those of (η^5:1-$Me_3SiC_9H_6$)$TiCl_3$ (**6**) and (η^5:C_9H_7)$TiCl_3$ (**5**). To investigate the position-dependent effect of the Me_3Si group, UV−vis spectroscopic and cyclic voltammetric studies were carried out. The results obtained give an insight into the relative energy levels of the frontier molecular orbitals of the respective indenyl titanium trichlorides. Quantum-chemical modeling studies were carried out on **4**−**6** to demonstrate the influence of the Me_3Si substituent effect with respect to the structural changes in the indenyl ligand and the Ti−D interaction (D = centroid of the five-membered ring of the indenyl moiety).

Introduction

Group 4 metal indenyl complexes are useful catalysts for homogeneous Ziegler−Natta olefin polymerization. For this reason, a large variety of indenyl-substituted complexes of this type have been synthesized.[1]

Recently, it has been shown that electron-withdrawing groups such as C_6F_5 in bis(cyclopentadienyl) and bis(indenyl) transition metal complexes significantly decrease the polymerization of ethene.[2] Based on this observation, the question arose, do electron-donating substituents such as Me and Me_3Si on the indenyl ligand increase the catalytic activity of the corresponding transition metal complexes?

We report here our study of the electronic effects of the Me_3Si group in indenyl-$TiCl_3$ complexes.

The chemical and physical properties of (η^5:2-$Me_3SiC_9H_6$)$TiCl_3$ are compared with those of (η^5:C_9H_7)$TiCl_3$ and (η^5:1-$Me_3SiC_9H_6$)$TiCl_3$.

Results and Discussion

Synthesis and Characterization. The half-sandwich complex (η^5:2-$Me_3SiC_9H_6$)$TiCl_3$ (**4**) was prepared in a three-step synthesis starting with 2-BrC_9H_7 (**1**) as outlined in Scheme 1.[3]

Scheme 1. Synthesis of 4

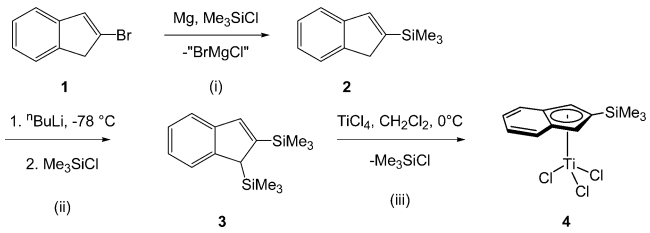

The regioselective formation of **4** is closely related to the different stabilization effects of the Me_3Si entity in position 1 or 2 in **3** (see below), which means that $TiCl_4$ preferentially reacts with the C(sp^3)−Si bond in position 1, rather than with the C(sp^2)−Si unit in position 2.

Complex **4** is soluble in common organic solvents except *n*-pentane; however, it appeared that it readily decomposes in tetrahydrofuran solutions even in absence of air. As usual for indenyltitanium trichlorides, solutions containing **4** are dark red-purple. Single crystals of **4** were obtained at −25 °C from dichloromethane. Solid **4** is readily oxidized in air, but is stable at low temperature under an inert gas atmosphere.

As typical for indenyltitanium trichloride species, two very distinctive absorptions are observed at 405 and 541 nm with ϵ = 1070 and 630 L cm^{-1} mol^{-1} in the UV−vis spectrum, of which the latter absorption is attributed to a ligand−metal CT transition.[4]

The reversible Nernst potential for **4** in cyclic voltammetric studies is found at E_0 = −0.92 V with ΔE = 180 mV. As demonstrated recently, UV−vis spectroscopic and cyclic voltammetric data can be used to study the position-dependent influence of substituents on

* To whom correspondence should be addressed. E-mail: heinrich.lang@chemie.tu-chemnitz.de.
† Present address: Technische Universität Bergakademie Freiberg, Fakultät für Chemie und Physik, Institut für Anorganische Chemie, Leipziger Strasse 29, D-09596 Freiberg/Sachsen, Germany.

(1) (a) Foster, P.; Chien, J. C. W.; Rausch, M. D. *J. Organomet. Chem.* **1997**, *527*, 71. (b) Foster, P.; Chien, J. C. W.; Rausch, M. D. *Organometallics* **1996**, *15*, 2404. (c) Kim, Y. *J. Organomet. Chem.* **1997**, *527*, 155. (d) Ready, T. E.; Day, R. O.; Chien, J. C. W.; Rausch, M. D. *Macromolecules* **1993**, *26*, 5822. (e) Ready, T. E.; Chien, J. C. W.; Rausch, M. D. *J. Organomet. Chem.* **1999**, *583*, 11. (f) Blais, M. S.; Chien, J. C. W.; Rausch, M. D. *Organometallics* **1998**, *17*, 3775.

(2) Maldanis, R. J.; Chien, J. C. W.; Rausch, M. D. *J. Organomet. Chem.* **2000**, *599*, 107.

(3) (a) Rakita, P. E.; Taylor, G. A. *Inorg. Chem.* **1972**, *9*, 2136. (b) Davison, A.; Rakita, P. *J. Organomet. Chem.* **1970**, *23*, 407. (c) Davison, A.; Rakita, P. E. *J. Organomet. Chem.* **1970**, *21*, 55.

(4) Weiss, T.; Karuppanan, N.; Lang, H.; Holze, R. *J. Electroanal. Chem.* **2002**, *533*, 127.

10.1021/om0400898 CCC: $30.25
Publication on Web 04/28/2005

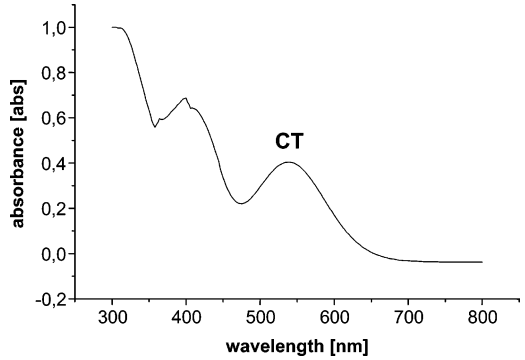

Figure 1. UV−vis spectrum of **6** (in dichloromethane).

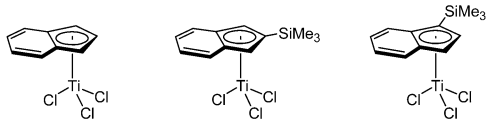

	5	4	6
λ_{max} [nm]	528 (2.35 eV)	541 (2.29 eV)	538 (2.30 eV)
ε [Lcmmol^{-1}]	936	630	1051

Figure 2. Comparison of the CT transitions of **4**−**6** (in dichloromethane).

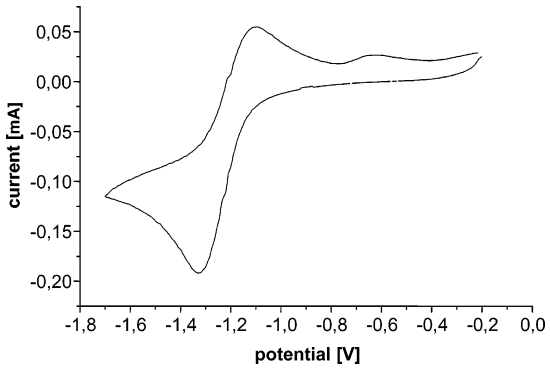

Figure 3. Cyclovoltammogram of **6** (in dichloromethane, referenced to the Cp_2Fe/Cp_2Fe^+ couple).

indenyl ligands.[4] In this respect, we compare here complex **4** with (η^5:C_9H_7)$TiCl_3$ (**5**) and (η^5:1-$Me_3SiC_9H_6$)-$TiCl_3$ (**6**) toward their (i) long-wave CT absorption maximum (UV−vis), (ii) reduction potential (cyclovoltammetry), (iii) structural properties (X-ray structure analysis), and (iv) quantum-chemical calculations.

UV−Vis Studies. Like **4**, complexes **5** and **6** show a representative CT transition at 528 (**5**) and 538 nm (**6**), respectively, in their UV−vis spectra. The UV−vis spectrum of **6** is illustrated in Figure 1.

As seen in Figure 2, **4** and **6** show their respective transitions red-shifted by ca. 10 nm, relative to **5**. Obviously, **4** and **6** show no position-dependent effect, since almost identical λ_{max} values are observed. The molar extinction coefficients with 600−1050 L cm^1 mol^{-1} are in the range typical for indenyltitanium trichlorides.

Cyclovoltammetric Studies. The reduction potentials of **4**−**6** were identified by cyclic voltammetric studies. The cyclovoltammogram of **6** is depicted in Figure 3. As typical for this type of complex a reversible redox process for the Ti(IV)/Ti(III) couple was found at E_{red} = −0.94 V (**5**), −1.01 V (**4**), and −1.34 V (**6**) with ΔE values being 234 mV (**5**), 180 mV (**4**), and 170 mV (**6**) (Figure 4).

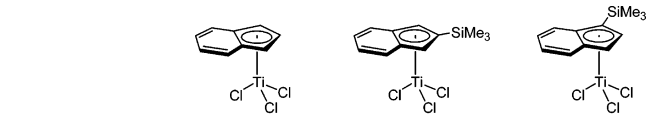

Standart Ti(IV)/Ti(III) potential vs. FcH/FcH$^+$(0.00 V)	5	4	6
E_{red} [V]	-0.94	-1.01	-1.34

Figure 4. E_{red} [V] values of complexes **4**−**6** (measured in dichloromethane solution; referenced to the Cp_2Fe/Cp_2Fe^+ couple).

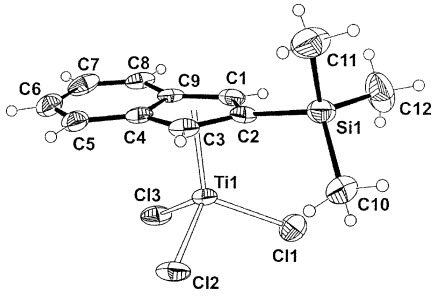

Figure 5. XP-plot (50% probability level) of **4** and the atom-numbering scheme.

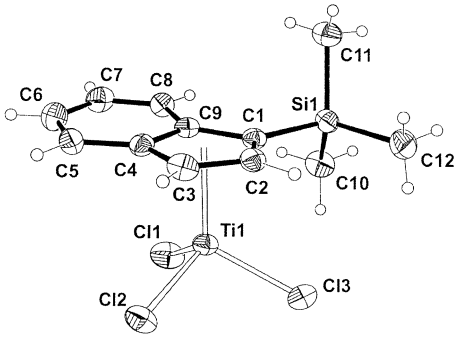

Figure 6. XP-plot (50% probability level) of **6** and the atom-numbering scheme.

The E_{red} potentials can be related to the LUMO energy levels. Both trimethylsilyl-substituted complexes **4** and **6** possess a more negative E_{red} value compared with **5**, indicating a more difficult reduction, due to the electron-donating effect of these groups (Figure 4). Furthermore, comparison of **4** with **6** demonstrates that there is also a significant position-dependent effect found for the Me_3Si substituents. When a Me_3Si substituent is in position 1, the reduction is more difficult than when the Me_3Si group is in position 2. A Me_3Si substituent in position 1 possesses better electron-donating properties than one in position 2.

X-ray Structure Analysis. The molecular solid-state structures of **4** (Figure 5) and **6** (Figure 6) are confirmed by X-ray structure analysis. Selected geometrical details are listed in Table 1, and crystallographic data are given in Table 2. The main characteristic feature of **4** is the piano-stool-like arrangement with the titanium atom Ti(1) in a pseudo-tetrahedral environment (Figure 1, Table 1). The η^5-coordination of the five-membered ring (C(1)−C(4), C(9)) to Ti(1) induces a butadiene-like structure in the six-membered cycle (C(4)−C(9)), which is characteristic for indenyl transition metal complexes and is also found for (η^5:C_9H_7)$TiCl_3$ (**5**) (Table 1).[5]

(5) Ready, T. E.; Day, R. O.; Chien, J. C. W.; Rausch, M. D. *Macromolecules* **1993**, *26*, 5822.

Table 1. Selected Bond Distances [Å] and Angles [deg] of Complexes 4−6[a]

	4	5[5]	6
	Bond Distances		
Ti(1)−D$_1$	2.027(2)	2.032(3)	2.057(2)
Ti(1)−Cl(1)	2.230(1)	2.231(2)	2.248(1)
Si(1)−C(1)/C(2)	1.878(4)	1.889(4)	
C(1)−C(4),C(9) av	1.422(4)	1.401(3)	1.436(4)
C(5)−C(6)	1.340(6)	1.359(2)	1.371(6)
C(6)−C(7)	1.422(6)	1.402(2)	1.403(7)
C(7)−C(8)	1.346(6)	1.338(2)	1.373(6)
	Bond Angles		
Cl(1)−Ti(1)−D$_1$	115.80(3)	114.2(2)	118.80(2)
Cl(1)−Ti(1)−Cl(2)	102.03(5)	102.4(2)	102.81(5)

[a] The estimated standard deviations of the last significant digits are shown in parentheses.

Table 2. Crystal and Intensity Collection Data for 4 and 6

	4	6
empirical formula	$C_{12}H_{15}Cl_3SiTi$	$C_{12}H_{15}Cl_3SiTi$
chemical formula	$C_{12}H_{15}Cl_3SiTi$	$C_{12}H_{15}Cl_3SiTi$
molecular mass	341.58	341.58
cryst syst	monoclinic	triclinic
space group	$P2(1)/c$	$P\bar{1}$
a (Å)	a = 18.4037(15) Å	a = 8.3259(6) Å
b (Å)	b = 6.7244(5) Å	b = 9.2701(7) Å
c (Å)	c = 12.4163(10) Å	c = 11.2872(9) Å
α (deg)	α = 90°	α = 68.261(2)°
β (deg)	β = 97.774(2)°	β = 87.679(2)°
γ (deg)	γ = 90°	γ = 75.007(2)°
V (Å^3)	1522.4(2) Å^3	780.18(10) Å^3
ρ_{calc} (g cm^{-3})	1.490 g/cm^3	1.454 g/cm^3
F(000)	696	348
Z	4	2
cryst dimens (mm^3)	0.55 × 0.5 × 0.04	0.4 × 0.35 × 0.02
radiation (λ, Å)	0.71073	0.71073
max., min. transmn	0.740232 and 0.522603	0.808978 and 0.567557
abs coeff (μ, mm^{-1})	1.143	1.115
temp (K)	173(2)	173(2)
scan mode	ω scans	σ scans
scan range (deg)	3.23−30.63	1.95−30.06
index ranges	$-25\le h\le 9$, $-8\le k\le 9$, $-8\le l\le 17$	$-11\le h\le 10$, $-12\le k\le 11$, $-14\le l\le 15$
	empirical	empirical
total no. of reflns	6854	5156
no. of unique reflns	3546	3665
no. of obsd reflns	2239	2110
$[I \ge 2\sigma(I)]$	0.0509	0.0430
completeness to θ max	75.5%	80.2%
no. of refined params	157	214
R1, wR2 $[I \ge 2\sigma(I)]$[a]	R1 = 0.0542, wR2 = 0.1048	R1 = 0.0519, wR2 = 0.0977
R1, wR2 (all data)[b]	R1 = 0.1019, wR2 = 0.1210	R1 = 0.1106, wR2 = 0.1183
max., min. peak in final Fourier map (e Å^{-3})	0.649, −0.421	0.682, −0.519

[a] R1 = $[\sum(||F_o| - |F_c|)/\sum|F_o|]$; wR2 = $[\sum(w(F_o^2 - F_c^2)^2)/\sum(wF_o^4)]^{1/2}$; $w = 1/[\sigma^2(F_o^2) + (0.0450P)^2 + 0.6907P]$ with $P = [F_o^2 + 2F_c^2]/3$; $S = [\sum w(F_o^2 - F_c^2)^2]/(n - p)^{1/2}$. [b] R1 = $[\sum(||F_o| - |F_c|)/\sum|F_o|]$; wR2 = $[\sum(w(F_o^2 - F_c^2)^2)/\sum(wF_o^4)]^{1/2}$; $w = 1/[\sigma^2(F_o^2) + (0.0362P)^2 + 0.0000P]$ with $P = [F_o^2 + 2F_c^2]/3$; $S = [\sum w(F_o^2 - F_c^2)^2]/(n - p)^{1/2}$. n = number of reflections, p = parameters used.

A weak haptotropic shift from η^5 toward η^3 is observed (ring-slippage 0.146 Å (distance between the perpendicular projection of the titanium atom Ti(1) on the plane of the five-membered cycle and the ring centroid D$_1$)).[6]

All other interatomic bond distances and bond angles are in agreement with this type of structural motif.[7]

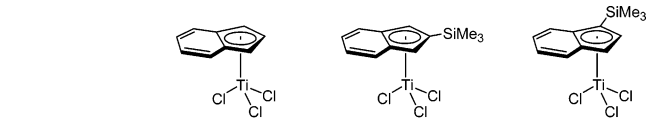

Figure 7. Comparison of Δ_c ([C−C] − [C=C]), Ti(1)−D$_1$, and ring slippage of complexes **4**−**6**.

The most representative feature of **6** (Figure 6) relating to **4** is the less pronounced haptotropic shift (0.111 Å) (Figure 7). This forces the carbon−carbon interatomic bond distances in the six-membered cycle (C(4)−C(9)) in such a way that C(5)−C(6) (1.371(6) Å) and C(7)−C(8) (1.373(6) Å) are somewhat elongated, while C(6)−C(7) (1.403(7) Å) is shortened when compared with **4** (Table 1). The difference between the average of the carbon−carbon double bonds (C(5)−C(6) and C(7)−C(8)) and the carbon−carbon single bond (C(6)−C(7)) in the six-membered indenyl unit goes along with the ring-slippage of the η^5-bound indenyl and the bond distance of the Ti(1)−D$_1$ separations (Figure 7).

Obviously, the Me$_3$Si substituent in position 1 (complex **6**) induces the smallest ring slippage and Δ_c value, but the longest Ti(1)−D$_1$ separation (Figure 7). This is associated with the strongest electron-donating effect of the Me$_3$Si group in position 1, which already was derived from the E_{red} data of **4**−**6** (see above).

Calculations

Quantum-chemical calculations have been carried out on **4**−**6**.[8] A fragment orbital analysis was performed with the extended Hückel method in order to obtain a deeper insight into the bonding properties of the indenyl-TiCl$_3$ complexes. The substitution of H by SiMe$_3$ in position 1 or 2 leads to a different orbital situation in the resulting molecules. The essential features of the orbital interaction between the Me$_3$Si and the (C$_9$H$_6$)-TiCl$_3$ fragments are shown in Figures 8 and 9. Molecules **4**−**6** have been arbitrarily divided into two radical fragments. The fragment orbital analysis of **4** (Figure 8) shows the interaction of FMO 76 (SOMO) with FMO 30, which forms the σ-bond (MO45). Furthermore, there is a weak interaction of FMO 77 with FMO 32. This represents a classical hyperconjugative interaction of a π-system with a σ-bonding Si−C orbital. The HOMO (MO43) and the LUMO (MO42) remain unaffected by Me$_3$Si substitution.

(6) For further theoretical and experimental studies see: (a) Calhorda, M. J.; Romao, C. C.; Veiros, L. F. *Chem. Eur. J.* **2002**, *8*, 868. (b) Martins, A. M.; Ascenso, J. R.; de Azevedo, C. G.; Calhorda, M. J.; Dias, A. R.; Rodrigues, S. S.; Toupet, L.; de Leonardis, P.; Veiros, L. F. *J. Chem. Soc., Dalton Trans.* **2000**, 4332.

(7) (a) Qian, Y.; Li, G.; Chen, W.; Li, B.; Youqi, T. *J. Organomet. Chem*. **1989**, *373*, 185. (b) Qichen, H.; Yonlong, Q.; Guisheng, L.; Youqi, T. *Transition Met. Chem*. **1990**, *15*, 483. (c) Flores, J. C.; Wood, J. S.; Chien, J. C. W.; Rausch, M. D. *Organometallics* **1996**, *15*, 4944. (d) Gallucci, J.; Kozmina, N.; Paquette, L. A.; Zaegel, F.; Meunir, P.; Gautheron, B. *Acta Crystallogr.* **1997**, *C53*, 1416. (e) Schneider, N.; Prosenc, M. H.; Brintzinger, H. H. *J. Organomet. Chem.* **1997**, *545*−*546,* 291.

(8) For further details see: Weiss, T. Indenyl-Metallkomplexe mit Metallen der Gruppe 4. Dissertation, TU Chemnitz, 2001, p 111. Accessible via the Internet at: http://archiv.tu-chemnitz.de/pub/2001/0057/data/weiss.pdf.

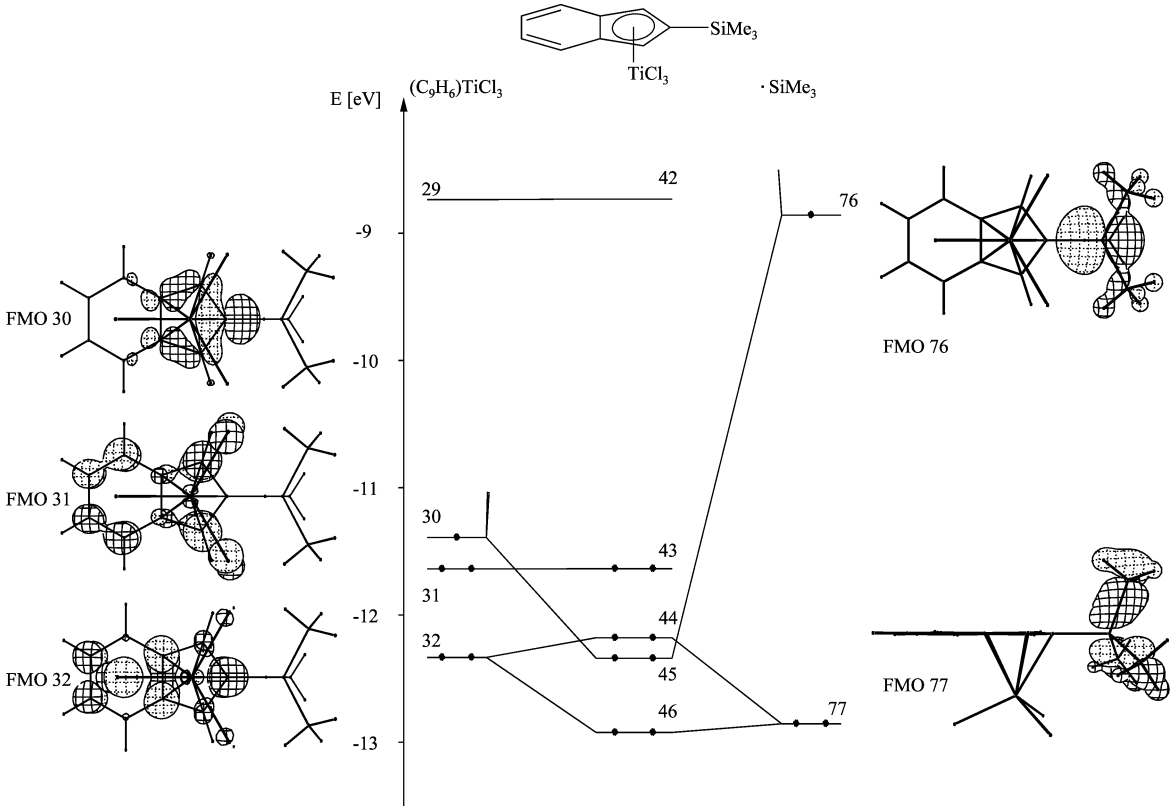

Figure 8. Orbital interaction diagram of **4**.

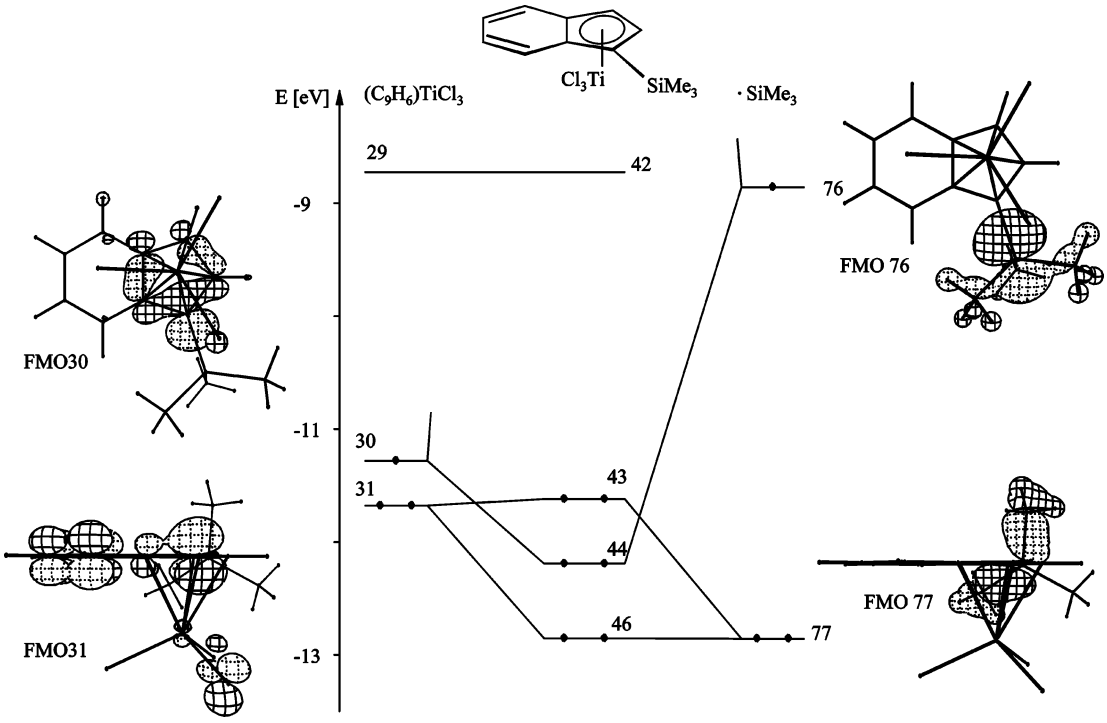

Figure 9. Orbital interaction diagram of **6**.

The bonding of the Me_3Si group in position 1 leads to a slightly different orbital interaction (Figure 9). FMO 76 forms with FMO 30 the σ-bond between the Me_3Si and the indenyl moiety. In addition, FMO 77 allows a hyperconjugative interaction with a π orbital of the $(C_9H_6)TiCl_3$ fragment. FMO 31 is suitable for this type of interaction, since the largest orbital coefficients are located at the carbon atoms 1 and 3, which means that the HOMO is affected by a hyperconjugative interaction with the Me_3Si group.

A Me_3Si substituent in position 1 of the indenyl group induces a substantial effect on the HOMO via hyperconjugative interaction, which explains the better electron-donating properties of the Me_3Si group in **6** compared to **4**.

Experimental Section

General Methods. All reactions were carried out in an atmosphere of purified nitrogen (O_2 traces: CuO catalyst, BASF AG, Ludwigshafen; H_2O: molecular sieve 4 Å) using standard Schlenk techniques. *n*-Pentane and dichloromethane were purified by distillation from calcium hydride. FT-IR spectra were recorded with a Perkin-Elmer FT-IR 1000 spectrometer as KBr pellets. UV−vis spectra were recorded with a Perkin-Elmer spectrometer (type Lambda 40) in dichloromethane as solvent (10^{-3} M) at 25 °C. NMR spectra were recorded with a Bruker Avance 250 spectrometer; ^{1}H NMR spectra were recorded at 250.130 MHz (internal standard relative to $CDCl_3$, δ = 7.27); $^{13}C\{^1H\}$ NMR spectra were recorded at 67.890 MHz (standard internal, relative to $CDCl_3$, δ 77.0). Chemical shifts are reported in δ units (ppm) downfield from $SiMe_4$ with the solvent signal as reference signal. Computational details: Extended Hückel calculations were performed with CACAO using the default atom parameters of the software package.[9] Molecules **4**, **5**, and **6** were constructed with idealized geometry following the data of the X-ray structure analyses (Ti−Cl 2.236 Å, Ti−D_1 (D_1 = centroid) 2.05 Å, idealized torsion angle Cl−Ti−D_1−C2 = 180°). Therefore, and because of the inherent simplifications of the EHT method, the orbital interaction diagrams (Figures 8 and 9) should be regarded as *qualitative pictures* of the bonding situation. Melting points were determined using analytically pure samples, sealed off in nitrogen-purged capillaries on a Gallenkamp MFB 595 010 M melting point apparatus. Microanalysis was performed by the Organic Department at Chemnitz, University of Technology.

General Remarks. Compounds **1**, **2**,[3] **3**,[10] **5**,[11] and **6**[1c] have been prepared by published procedures. All other chemicals were purchased by commercial suppliers and were used as received.

Synthesis of 4. 1,2-$(Me_3Si)_2C_9H_6$ (**3**) (0.48 g, 1.9 mmol) was dissolved in 10 mL of dichloromethane, and $TiCl_4$ (0.35 g, 0.21 mL, 1.9 mmol), dissolved in 5 mL of *n*-pentane, was added dropwise at −10 °C. After 20 h of stirring at 25 °C, the initially colorless reaction mixture became red. Subsequently, all volatile materials were removed in a vacuum, and the residue was extracted with 3 × 3 mL of *n*-pentane. After addition of 30 mL of dichloromethane, the solution was filtered through a pad of Celite. Evaporation of the solvents in a vacuum gave a dark red solid, soluble in *n*-pentane and diethyl ether. Single crystals of **4** were obtained by slowly cooling a dichloromethane solution at −25 °C. Yield: 0.47 g (1.37 mmol, 74% basen on **3**), mp 126 °C. Anal. Calcd for $C_{12}H_{15}Cl_3SiTi$ (341.59): C, 42.19; H, 4.43. Found: C, 41.91; H, 4.65. IR [cm^{-1}]: 3083 (m), 2957 (m), 2898 (w), 1947 (w), 1811 (w), 1756 (w), 1607 (m, br), 1445 (m), 1406 (m), 1338 (m), 1273 (m), 1246 (s), 1088 (s), 920 (s), 881 (s), 843 (vs), 751 (s), 701 (m). ^{1}H NMR ($CDCl_3$): δ 0.44 (s, 9 H, $SiMe_3$), 7.39 (s, 2 H, C_9H_6), 7.55 (dd, $^2J_{HH}$ = 7.4 Hz, $^3J_{HH}$ = 3.5 Hz, C_9H_6), 7.79 (dd, 2 H, $^2J_{HH}$ = 7.4 Hz, $^3J_{HH}$ = 3.5 Hz, C_9H_6). $^{13}C\{^1H\}$ NMR ($CDCl_3$): δ −0.6 ($SiMe_3$), 122.6 (CH, C_9H_4), 127.4 (CH, C_9H_4), 130.2 (CH, C_6H_5), 135.1 (^iC, C_9H_4), 145.1 (C−Si, C_9H_5). UV−vis (CH_2Cl_2; λ_{max} (nm) (ϵ, 1.0 cm^{-1} mol^{-1})): 405 (1072), 541 (630). CV (CH_2Cl_2; $E°$ (ΔE) in V): −0.92 (0.09).

X-ray Structure Determination of 4 and 6. The solid-state structures of **4** and **6** were determined by single-crystal X-ray diffraction. Data collection was performed on a Siemens-Stoe AED2 diffractometer using Mo Kα radiation (graphite monochromator). Crystallographic data of **4** and **6** are given in Table 2. The structure was solved by direct methods (SHELX 97; Sheldrick, G. M. University of Göttingen: Göttingen, Germany, 1997). A semiempirical absorption correction based on φ-scans was applied. The structure was refined by the least-squares method based on F^2 with all reflections. All non-hydrogen atoms were refined anisotropically; the hydrogen atom positions have been taken from the difference Fourier map and refined freely.

Acknowledgment. We are grateful to Bayer AG Leverkusen for financial support. Special thanks are given to the Computing Center of the TU Bergakademie Freiberg for supplying disk space and computing time.

Supporting Information Available: Details about the X-ray crystal structures, including diagrams, and tables of crystal data and structure refinement, atomic coordinates, bond lengths and angles, and anisotropic displacement parameters for **4** and **6**. This material is available free of charge via the Internet at http://pubs.acs.org.

OM0400898

(9) Mealli, C.; Proserpio, D. M. *J. Chem. Educ.* **1990**, *67*, 399.
(10) (a) Billups, W. *J. Org. Chem.* **1980**, *23*, 4638. (b) Porter, H. D.; Suter, C. M. *J. Am. Chem. Soc.* **1935**, *57*, 2022.
(11) Cardoso, A. M.; Clark, R. J. H.; Moorhouse, S. *J. Chem. Soc., Dalton Trans.* **1976**, 707.